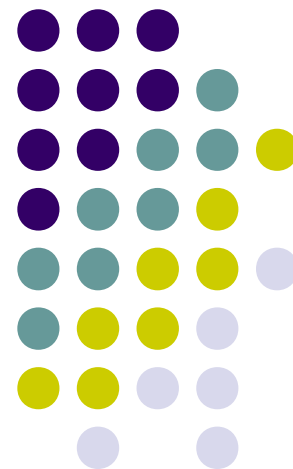


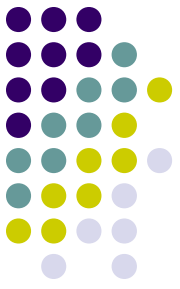
Ionization Dynamics of Atoms Exposed to Strong Laser Pulses: Semi-Analytical Model at Low Field Frequencies

Yu.V. Popov

Skobeltsyn Institute of Nuclear Physics,
Lomonosov Moscow State University

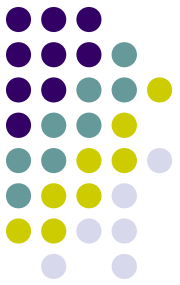


Collaboration



- **B. Piraux, A. Hamido**. Inst. of Condensed Matter and Nanosciences, Universite catolique de Louvain, Louvain-la-Neuve, Belgium
- **H. M. Tetchou Nganso**. CEPAMOQ, Faculty de Science, University of Douala, Douala, Cameroon
- **A. G. Galstyan**. Faculty of Physics, Lomonosov Moscow State University, Moscow, Russia
- **O. Chuluunbaatar**. LIT, JINR, Dubna, Russia
- **F. Mota-Furtado, P. O'Mahony**. Department of Mathematics, Royal Holloway, University of London, Egham, United Kingdom

INTRODUCTION AND MOTIVATIONS



The study of the highly nonlinear interaction of one-electron atoms with intense **infrared** laser pulses has stimulated the development of numerous mathematical methods and numerical algorithms to solve the corresponding time-dependent Schrödinger equation (TDSE).

INTRODUCTION AND MOTIVATIONS



Keldysh has introduced the adiabaticity parameter

$$\gamma = \omega(2I_p)^{1/2}/E$$

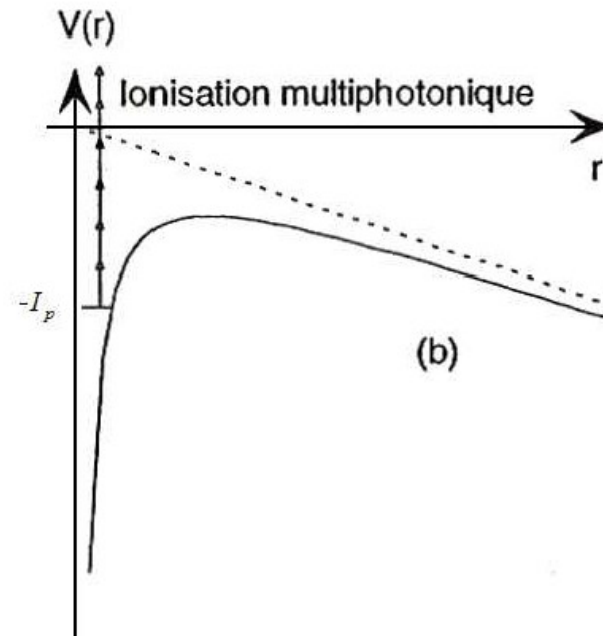
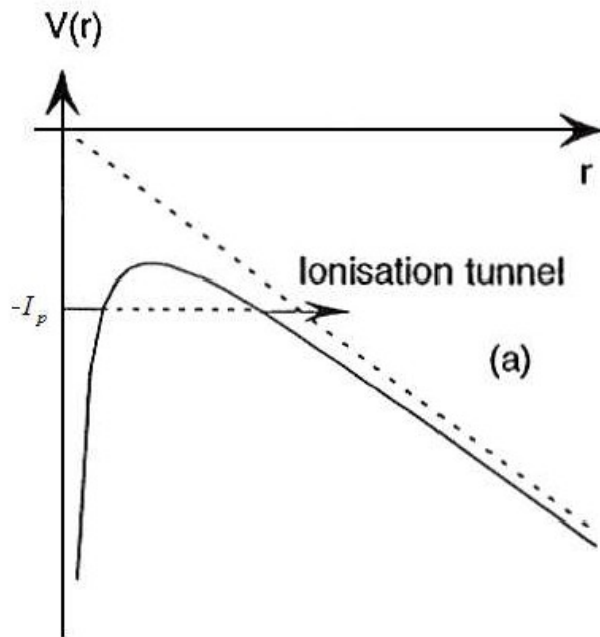
where ω is the laser field frequency, E , the field amplitude, and I_p the ionization potential of the atom.

For $\gamma > 1$, ATI and harmonic generation occur via multiphoton transitions while in the strong field limit.

For $\gamma < 1$, tunnel ionization takes place.

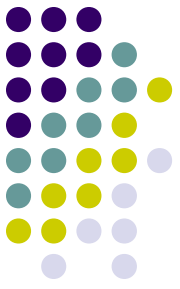
For Ti-Sapphire laser $E \sim 0.1$, $\omega = 0.057$, $I_p = 0.5$ for atomic hydrogen

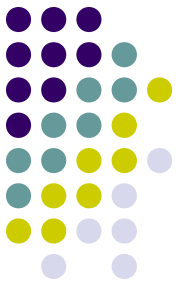
Two main mechanisms of ionization



INTRODUCTION AND MOTIVATIONS

For $\gamma < 1$, the electron can escape from the vicinity of the ion core by tunneling through the barrier formed by the Coulomb attraction of the core and the time-dependent electric field generated by the laser. Once the electron is released, it is driven back and forth by the external field. It can therefore experience multiple returns to the nucleus. When the electron gets back to the nucleus, it can be scattered by the ion core or recombine in the ground state of the atom leading to HOHG of the driving field.

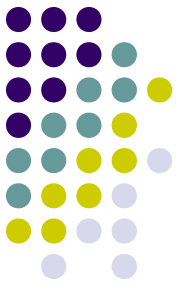




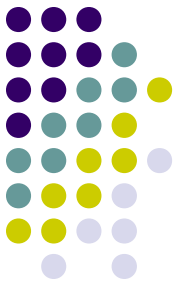
INTRODUCTION AND MOTIVATIONS

This picture is the basis of a well-known theoretical model, the so-called “strong field approximation” (SFA) where it is assumed that the dynamics are governed by the coupling of the ground state with the continuum and that the ejected electron is described by a Volkov state that ignores the presence of the Coulomb potential.

INTRODUCTION AND MOTIVATIONS

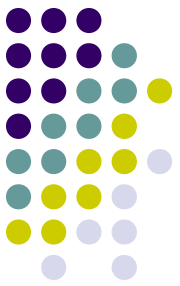


In fact, for $\gamma \ll 1$ and *a fortiori* for $\gamma \approx 1$, it is impossible to make a clear-cut separation between the two mechanisms. Both of them, multiphoton processes and tunnel ionization play a role. This has been confirmed experimentally and by numerical simulations. High-resolution fully differential experimental data on single ionization of rare gases (He, Ne, and Ar) by short laser pulses have been obtained by Rudenko *et al.* **Their data clearly show that deep in the tunneling regime, the low-energy ATI peaks exhibit a fine structure that is unambiguously attributed to a resonant multiphoton process.**



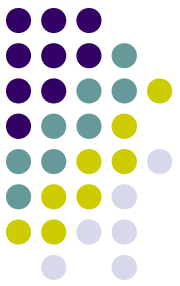
MAIN PURPOSE OF OUR WORK :

These results raise the fundamental question of the actual role of the Coulomb potential in the intensity regime where tunnel ionization is supposed to take place. **In order to address this question, we have developed a model calculation which goes far beyond the SFA. It is this mathematical model that we present in this contribution.**



The main idea of the present approach is to substitute in momentum space, the kernel of the nonlocal Coulomb potential by a sum of N separable potentials, each of them supporting one bound state of atomic hydrogen. This approach which is widely used in nuclear physics for short-range potentials, allows one to reduce the 3D TDSE to a system of N coupled 1D linear Volterra integral equations of the second kind that we solve numerically. The model presents several advantages:

- it provides a rigorous solution for the electron wave packet;
- by contrast with the SFA, more than one bound state may be included in the model;
- the continuum-continuum dipole matrix elements are treated exactly;
- the theory is fully gauge invariant.

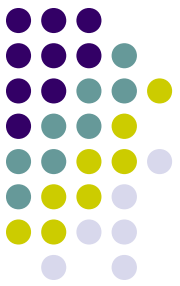


BRIEF SUMMARY OF THE THEORY

SE in the momentum space

$$\left[i \frac{\partial}{\partial t} - \frac{p^2}{2} - \frac{1}{c} A(t) (\vec{e} \cdot \vec{p}) \right] \Phi(\vec{p}, t) - \int \frac{d\vec{p}'}{(2\pi)^3} V(\vec{p}, \vec{p}') \Phi(\vec{p}', t) = 0.$$

$$A(t) = A_0 f(t) \sin(\omega t + \phi) \quad f(t) = \begin{cases} \sin^2(\pi t/T), & 0 \leq t \leq T, \\ 0, & t > T, \end{cases}$$



SEPARABLE POTENTIALS

$$V(\vec{p}, \vec{p}') = - \sum_{n=1}^N v_n(\vec{p}) v_n^*(\vec{p}')$$

$$\left(\varepsilon_j - \frac{1}{2} p^2 \right) \varphi_j(\vec{p}) + \sum_{n=1}^N a_{jn} v_n(\vec{p}) = 0$$

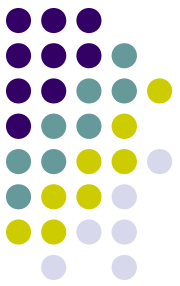
$$a_{jn} = \int \frac{d\vec{p}'}{(2\pi)^3} v_n^*(\vec{p}') \varphi_j(\vec{p}')$$

$$\gamma_{ij} = - \int \frac{d\vec{p}}{(2\pi)^3} \varphi_i^*(\vec{p}) \left(\varepsilon_j - \frac{1}{2} p^2 \right) \varphi_j(\vec{p})$$

$$\Phi = -\mathbf{A}\mathbf{V}$$

$$\mathbf{V} = -\mathbf{A}^{-1}\Phi$$

$$\mathbf{\Gamma} = \mathbf{A}\mathbf{A}^T;$$

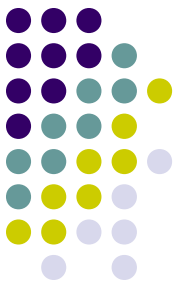


The elements of the Γ -matrix are the first to be calculated analytically.

For the hydrogen atom, the matrix of the potential is a block-diagonal :

$$V(\vec{p}, \vec{p}') = -V^{(s)}(\vec{p}, \vec{p}') - V^{(p)}(\vec{p}, \vec{p}') - V^{(d)}(\vec{p}, \vec{p}') - \dots$$

$$V^{(l)}(\vec{p}, \vec{p}') = \sum_{j=1}^{N_l} v_j^{(l)}(p) v_j^{(l)}(p') (Y_l(\vec{p}) \cdot Y_l(\vec{p}'))$$



CONTINUUM SPECTRUM

$$\left(E - \frac{p^2}{2}\right) \tilde{\Phi}^-(\vec{k}, \vec{p}, \vec{R}) + \sum_{i=1}^N C_i(\vec{k}) v_i(\vec{p}, \vec{R}) = 0, \quad E = k^2/2,$$

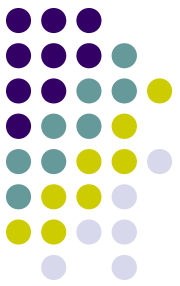
$$C_i(\vec{k}) = \int \frac{d\vec{p}}{(2\pi)^3} v_i^*(\vec{p}, \vec{R}) \tilde{\Phi}^-(\vec{k}, \vec{p}, \vec{R})$$

$$\tilde{\Phi}^-(\vec{k}, \vec{p}, \vec{R}) = (2\pi)^3 \delta(\vec{k} - \vec{p}) - \frac{1}{(E - p^2/2 - i0)} \sum_i C_i(\vec{k}) v_i(\vec{p}, \vec{R})$$

$$C_i(\vec{k}) [1 + \lambda_{ii}(k)] + \sum_{i \neq j}^N \lambda_{ij}(k) C_j(\vec{k}) = v_i^*(\vec{k}, \vec{R})$$

$$\lambda_{ij}(k) = \int \frac{d\vec{p}}{(2\pi)^3} \frac{v_i^*(\vec{p}, \vec{R}) v_j(\vec{p}, \vec{R})}{E - p^2/2 - i0}.$$

also to be calculated analytically



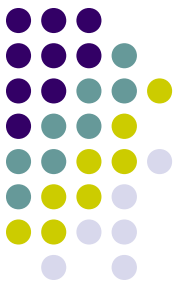
SOLUTION OF THE TDSE IN MOMENTUM SPACE

$$\left[i \frac{\partial}{\partial t} - \frac{p^2}{2} + (\vec{e} \cdot \vec{p}) \frac{\partial}{\partial t} b(t) \right] \tilde{\Phi}(\vec{p}, \vec{R}, t) + \sum_{n=1}^N v_n(\vec{p}, \vec{R}) F_n(\vec{R}, t) = 0$$

$$F_j(\vec{R}, t) = \int \frac{d\vec{p}}{(2\pi)^3} v_j^*(\vec{p}, \vec{R}) \tilde{\Phi}(\vec{p}, \vec{R}, t)$$

$$b(t) = -(1/c) \int_0^t A(\tau) d\tau \quad \tilde{\Phi}(\vec{p}, \vec{R}, 0) = \tilde{\Phi}_{HOMO}(\vec{p}, \vec{R})$$

$$\tilde{\Phi}(\vec{p}, \vec{R}, t) = \exp[-itp^2/2 + ib(t)(\vec{e} \cdot \vec{p})] \left[\tilde{\Phi}_{HOMO}(\vec{p}, \vec{R}) + \right. \\ \left. i \sum_{n=1}^N \int_0^t d\tau v_n(\vec{p}, \vec{R}) F_n(\tau) \exp[i\tau p^2/2 - ib(\tau)(\vec{e} \cdot \vec{p})] \right]$$



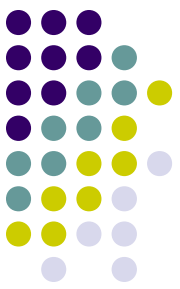
We obtain a system of time-dependent linear Volterra integral equations which can be written in matrix form as follows:

$$\mathbf{F}(\vec{R}, t) = \mathbf{F}_0(\vec{R}, t) + \int_0^t \mathbf{K}(\vec{R}; t, \tau) \mathbf{F}(\vec{R}, \tau) d\tau,$$

$$F_{i0}(\vec{R}, t) = \int \frac{d\vec{p}}{(2\pi)^3} v_i^*(\vec{p}, \vec{R}) \tilde{\Phi}_1(\vec{p}, \vec{R}) e^{-itp^2/2 + ib(t)(\vec{e} \cdot \vec{p})},$$

$$K_{in}(\vec{R}; t, \tau) = i \int \frac{d\vec{p}}{(2\pi)^3} v_i^*(\vec{p}, \vec{R}) v_n(\vec{p}, \vec{R}) e^{-i(t-\tau)p^2/2 + i[b(t) - b(\tau)](\vec{e} \cdot \vec{p})}$$

We can introduce the new analytical element



$$S_{kl}(\xi, \eta) = \int \frac{d\vec{p}}{(2\pi)^3} \tilde{\Phi}_k^*(\vec{p}, \vec{R}) \tilde{\Phi}_l(\vec{p}, \vec{R}) e^{-i\xi p^2 + i\eta(\vec{e} \cdot \vec{p})}$$

$$F_{i0}(\vec{R}, t) = \sum_{k=1}^N a_{ik}^{-1} \left(\varepsilon_k - i \frac{1}{2} \frac{\partial}{\partial \xi} \right) S_{k1}(\xi, \eta)_{(\xi=t/2, \eta=b(t))}$$

$$K_{in}(\vec{R}; t, \tau) = i \sum_{k,m=1}^N a_{ik}^{-1} a_{nm}^{-1} \left(\varepsilon_k - i \frac{1}{2} \frac{\partial}{\partial \xi} \right) \left(\varepsilon_m - i \frac{1}{2} \frac{\partial}{\partial \xi} \right) S_{km}(\xi, \eta)_{(\xi=(t-\tau)/2, \eta=b(t)-b(\tau))}$$



The main 3D integrals can be calculated analytically. We then solve the system of 1D coupled Volterra equations on grid, calculate the wave- packet, and then calculate various differential probabilities.

Results and their interpretation

For the bound state $\langle v_z \rangle \approx 0$

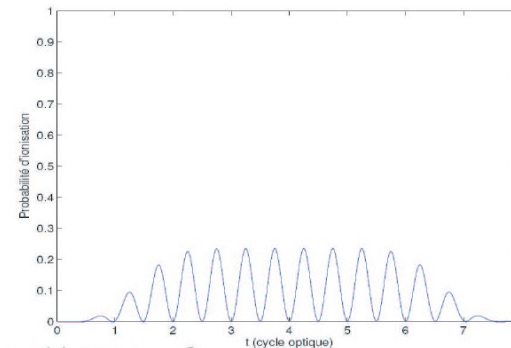
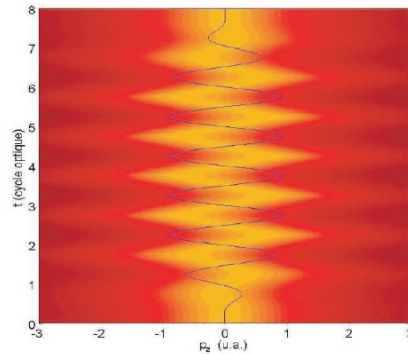
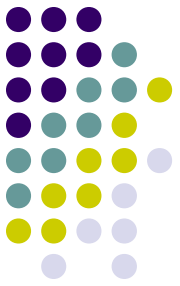
$$\vec{v} = \vec{p} + e\vec{A}(t), \quad \langle p_z \rangle \approx -A(t)$$

The Ehrenfest's theorem (classic)

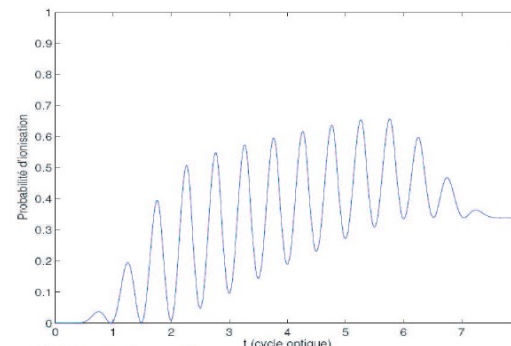
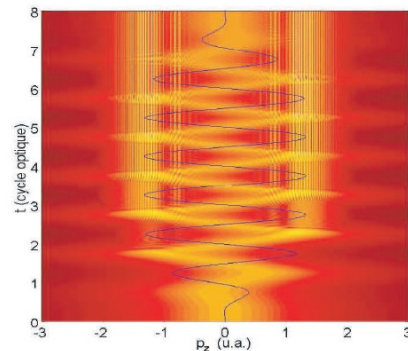
$$\frac{d}{dt} \langle \vec{p} \rangle = -(\vec{\nabla}V) - E(t)$$

being applied for the continuum states after end of the pulse

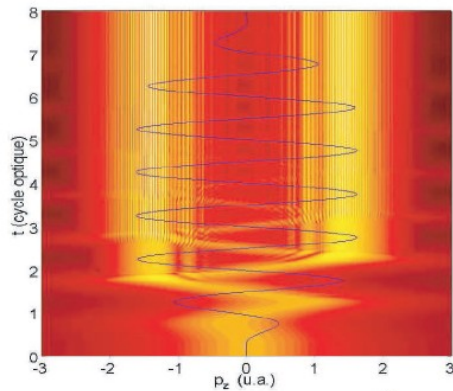
$$\frac{d}{dt} \langle \vec{p} \rangle = -(\vec{\nabla}V) \sim 0 \rightarrow \langle \vec{p} \rangle = \text{const}$$



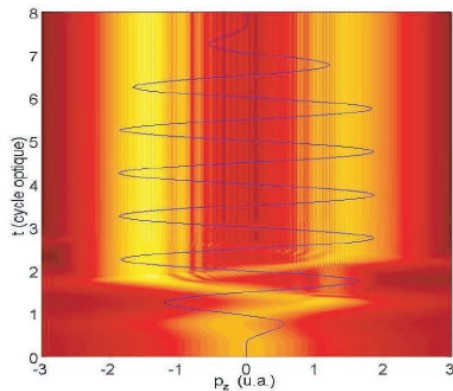
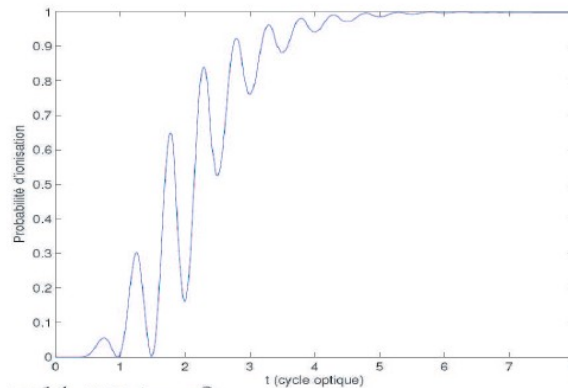
$$I = 1 \times 10^{14} \text{ W/cm}^2$$



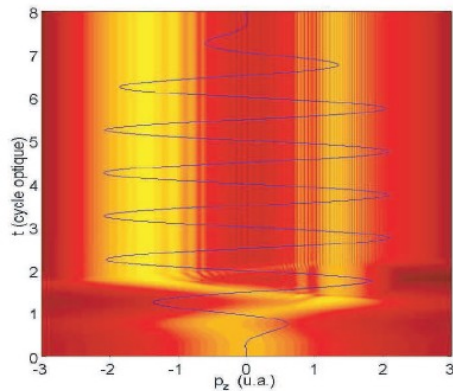
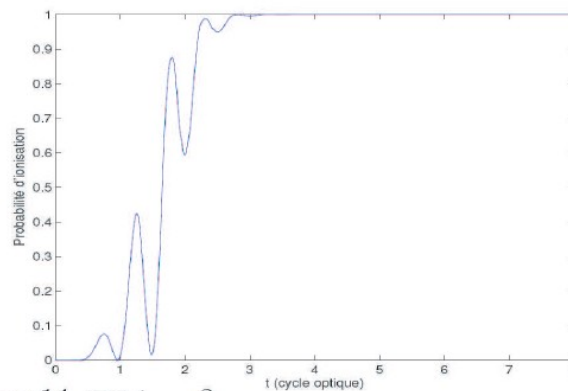
$$I = 2 \times 10^{14} \text{ W/cm}^2$$



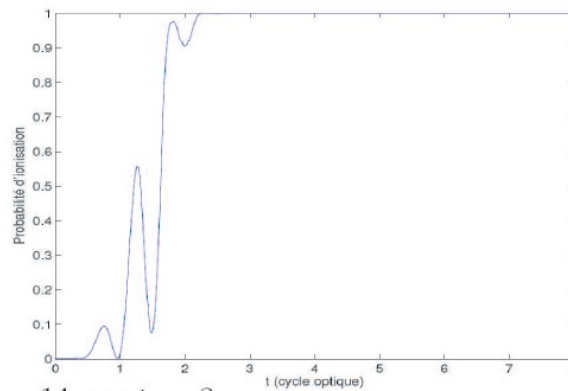
$$I = 3 \times 10^{14} \text{ W/cm}^2$$



$$I = 4 \times 10^{14} \text{ W/cm}^2$$



$$I = 5 \times 10^{14} \text{ W/cm}^2$$



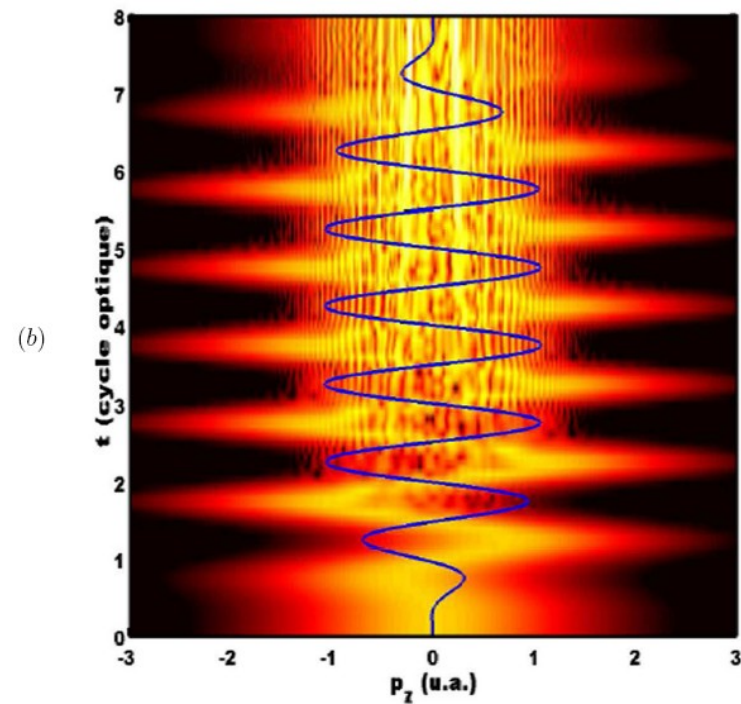
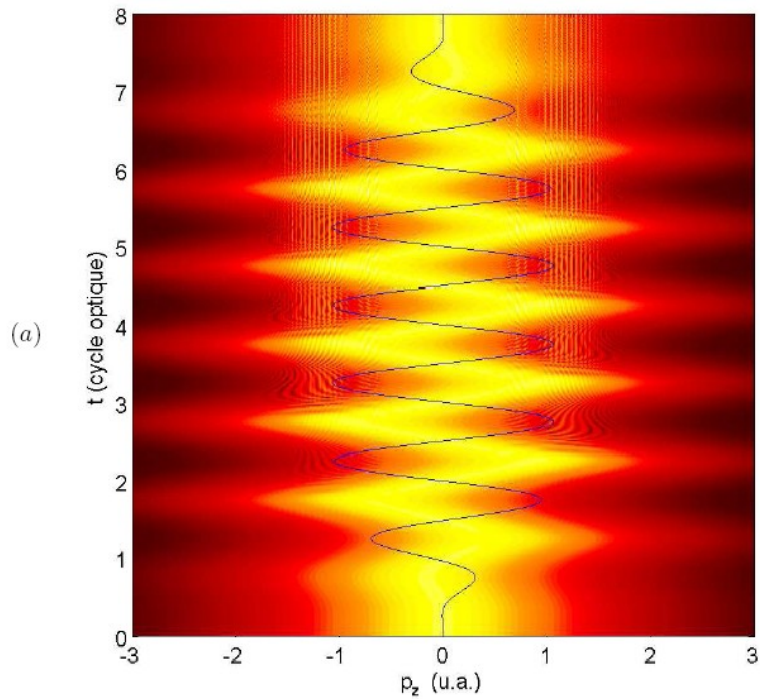
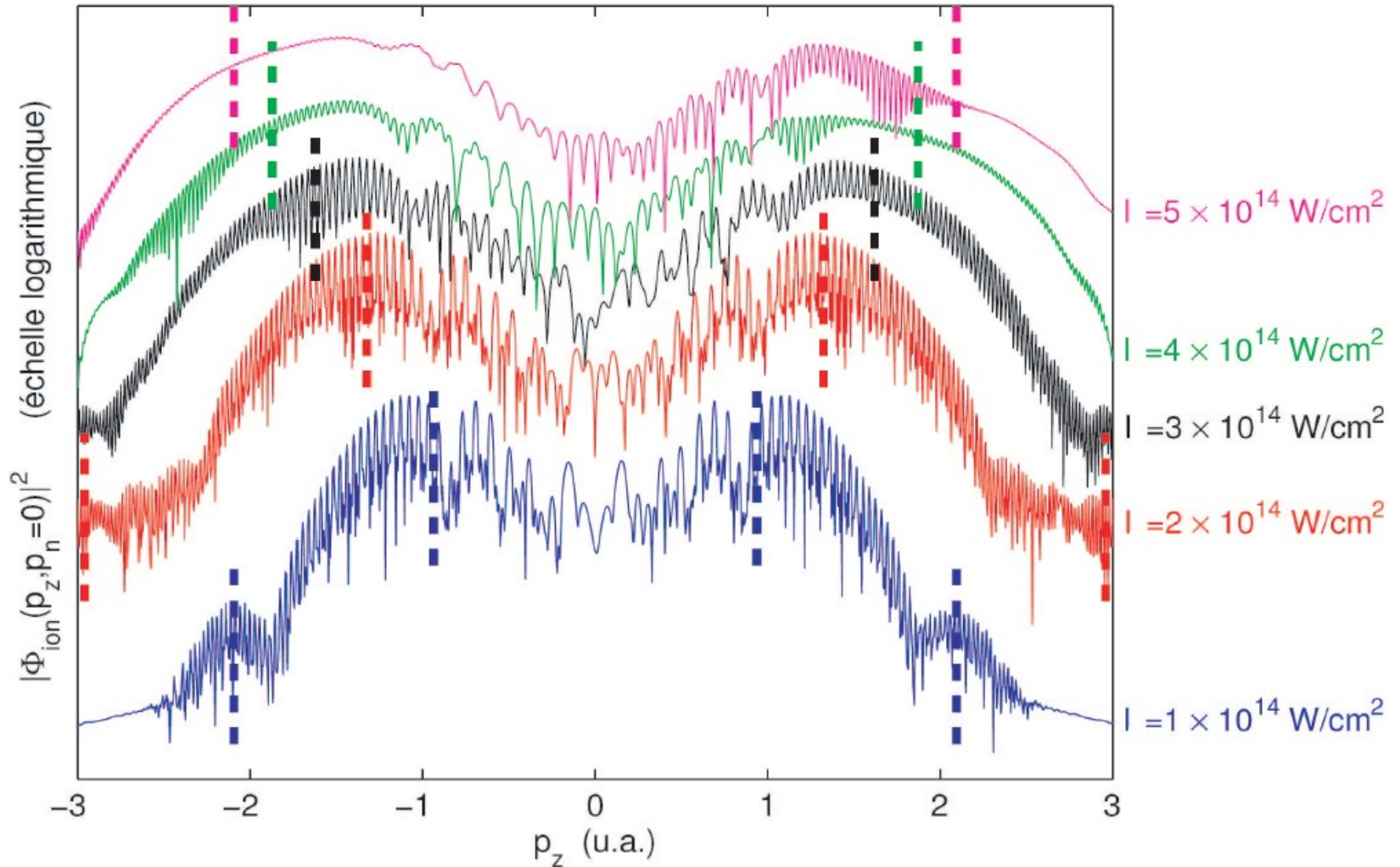
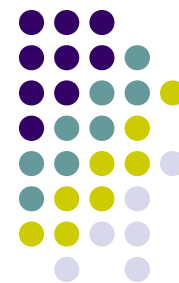
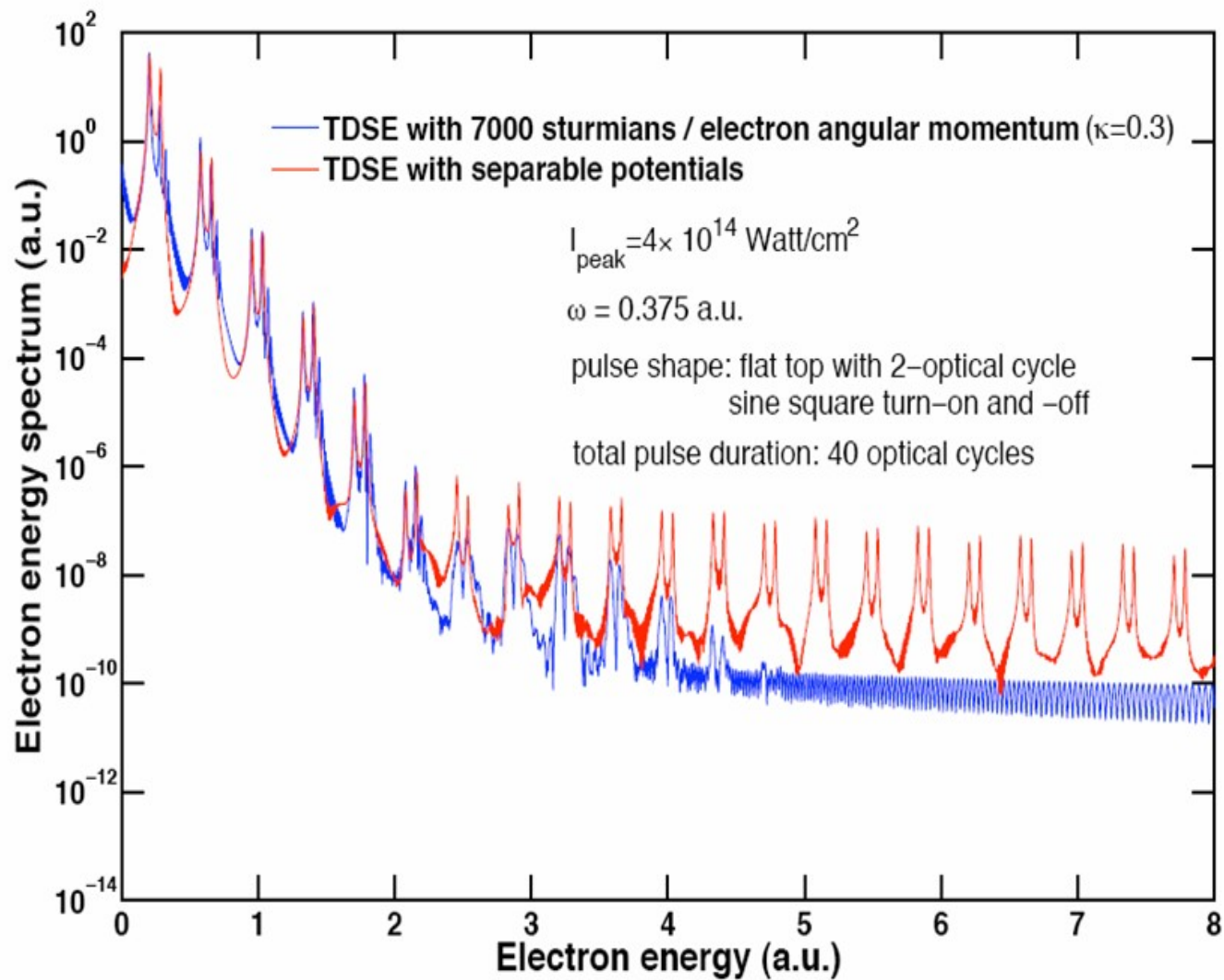


FIG. 3.6 – Densité de probabilité $|\Phi(p_n = 0, p_z, t)|^2$ en échelle logarithmique pour une interaction de 8 cycles optiques, une intensité de $1.3 \times 10^{14} \text{ W/cm}^2$ et une fréquence de 0.057 u.a. , avec notre nouveau modèle (a) et obtenue par A. de Bohan (b). Le potentiel vecteur $A(t)$ est superposé en bleu.

Between $2U_p < |p_z| < 10U_p$, we observe a qualitative agreement with the results of our calculations for the pure Coulomb potential.







КОНЕЦ

Спасибо за внимание !